Organic aerosol effects on fog droplet spectra

Yi Ming
Geophysical Fluid Dynamics Laboratory, Princeton, New Jersey, USA

Lynn M. Russell
Scripps Institution of Oceanography, University of California, San Diego, La Jolla, California, USA

Received 8 December 2003; revised 5 March 2004; accepted 17 March 2004; published 26 May 2004.

[1] Organic aerosol alters cloud and fog properties through surface tension and solubility effects. This study characterizes the role of organic compounds in affecting fog droplet number concentration by initializing and comparing detailed particle microphysical simulations with two field campaigns in the Po Valley. The size distribution and chemical composition of aerosol were based on the measurements made in the Po Valley Fog Experiments in 1989 and 1998–1999. Two types of aerosol with different hygroscopicity were considered: the less hygroscopic particles, composed mainly of organic compounds, and the more hygroscopic particles, composed mainly of inorganic salts. The organic fraction of aerosol mass was explicitly modeled as a mixture of seven soluble compounds [*Fuzzi et al.*, 2001] by employing a functional group-based thermodynamic model [*Ming and Russell*, 2002]. Condensable gases in the vapor phase included nitric acid, sulfuric acid, and ammonia. The maximum supersaturation in the simulation is 0.030% and is comparable to the calculation by *Noone et al.* [1992] inferred from measured residual particle fractions. The minimum activation diameters of the less and more hygroscopic particles are 0.49 μm and 0.40 μm, respectively. The predicted residual particle fractions are in agreement with measurements. The organic components of aerosol account for 34% of the droplet residual particle mass and change the average droplet number concentration by −10–6%, depending on the lowering of droplet surface tension and the interactions among dissolving ions. The hygroscopic growth of particles due to the presence of water-soluble organic compounds enhances the condensation of nitric acid and ammonia due to the increased surface area, resulting in a 9% increase in the average droplet number concentration. Assuming ideal behavior of aqueous solutions of water-soluble organic compounds overestimates the hygroscopic growth of particles and increases droplet numbers by 6%. The results are sensitive to microphysical processes such as condensation of soluble gases, which increases the average droplet number concentration by 26%. Wet deposition plays an important role in controlling liquid water content in this shallow fog. *INDEX TERMS:* 0305 Atmospheric Composition and Structure: Aerosols and particles (0345, 4801); 0320 Atmospheric Composition and Structure: Cloud physics and chemistry; *KEYWORDS:* aerosol-cloud interaction, fog, droplet spectra, organic aerosol, Po Valley, hygroscopic growth

Citation: Ming, Y., and L. M. Russell (2004), Organic aerosol effects on fog droplet spectra, *J. Geophys. Res.*, *109*, D10206, doi:10.1029/2003JD004427.

1. Introduction

[2] Aerosol particles in the atmosphere often consist of complex mixtures of inorganic and organic compounds [*Duce et al.*, 1983; *Rogge et al.*, 1993; *Middlebrook et al.*, 1998]. Soluble components enable particles to activate as cloud condensation nuclei (CCN) into cloud or fog droplets in meteorological conditions favorable for supersaturation. Droplets also include large haze particles that have taken up water at high relative humidity but have not exceeded critical diameters required for activation. One example of supersaturated conditions is water vapor condensing and growing aerosol particles into droplets forming radiative fog. High concentrations of particles and acidic gases (i.e., SO_2 and NO_2) are characteristic of polluted fog events in densely populated areas and have serious detrimental effects on human health [*Wyzga and Folinsbee*, 1995]. Studies of the chemical and microphysical processes in fog systems provide a better understanding of the role of fog in producing (by aqueous-phase oxidation of SO_2) and removing (by wet deposition) particulate matter [*Lillis et al.*, 1999].

[3] A significant fraction of aerosol mass (up to 70%) is composed of organic compounds, many of which lower droplet surface tension and dissolve in water [*Facchini et al.*, 2000]. Both effects increase the number of droplets

0148-0227/04/2003JD004427$09.00

formed in supersaturated conditions by decreasing the critical supersaturation relative to an equivalent mass of insoluble solid that neither coats nor dissolves in the particle. For the four hypothetical chemical compositions in Figure 1 (NO, No solubility Or surface tension; OS, Only Solubility; OT, Only surface Tension; ST, Solubility and surface Tension), droplet concentration increases due to the surface tension effect of organic components when insoluble inorganic compounds in the NO case are replaced by insoluble organic compounds in the OT case. The solubility effect of organic components increases droplet concentration further if organic compounds become soluble in the ST case. Laboratory and field measurements indicated that some ambient particles that are composed mainly of organic species are able to grow into droplets [*Cruz and Pandis*, 1997; *Corrigan and Novakov*, 1999; *Russell et al.*, 2000]. An equilibrium-based calculation showed that replacing part of the insoluble material in aerosol particles with soluble organic compounds increases CCN number concentrations by up to 13%, 97% and 110% for typical marine, rural and urban aerosols [*Mircea et al.*, 2002]. *Nenes et al.* [2002] used an adiabatic cloud parcel model with aerosol microphysics to study the effects of organic aerosol on cloud droplet number concentration, reporting that surface-active organic compounds can increase the droplet number concentration by as much as 53%. They also found that the likely suppression of the mass accommodation coefficient of water due to the presence of organic film forming compounds (FFC) [*Feingold and Chuang*, 2002] can either increase or decrease droplet numbers, depending on the initial size-resolved distributions.

[4] *Decesari et al.* [2000] proposed a new experimental technique to characterize water-soluble organic compounds with a combination of chromatographic separation, proton nuclear magnetic resonance (HNMR) and total organic carbon (TOC) analysis. On the basis of the quantitative measurements of organic carbon concentrations and HNMR-derived proton concentrations of four functional groups, seven model compounds commonly found in the atmosphere were selected to represent the chemical composition of water-soluble organic mass [*Fuzzi et al.*, 2001].

[5] In this study, we used an aerosol dynamic model with detailed microphysical processes to simulate fog events in a polluted rural area (Po Valley, Italy). The droplet surface tension was related to organic concentration using the measurements by *Facchini et al.* [2000]. The hygroscopicity of organic aerosol was calculated based on the chemical composition explicitly represented by the compounds suggested by *Fuzzi et al.* [2001] with the thermodynamic model developed by *Ming and Russell* [2002]. We examined the model sensitivity to condensation of soluble gases, hygroscopic growth and wet deposition. The surface tension and solubility effects of organic aerosol on fog droplet number concentration were also investigated.

2. Case Study and Model Description

[6] The Po Valley is a highly populated area affected by both agricultural and industrial pollution. Fog forms frequently during the fall-winter season (30% of the time) as a result of the ground-based temperature inversion favored by the surrounding mountain ranges [*Fuzzi et al.*, 1992]. The Po Valley Fog Experiment of 1989 was an extensive fog microphysics study at S. Pietro Capofiume in November 1990 [*Fuzzi et al.*, 1992]. The measured meteorological data included temperature, relative humidity (RH), liquid water content (LWC) and gas-phase concentrations of SO_2, NO, NO_2, HNO_3, NH_3 and O_3 [*Wobrock et al.*, 1992].

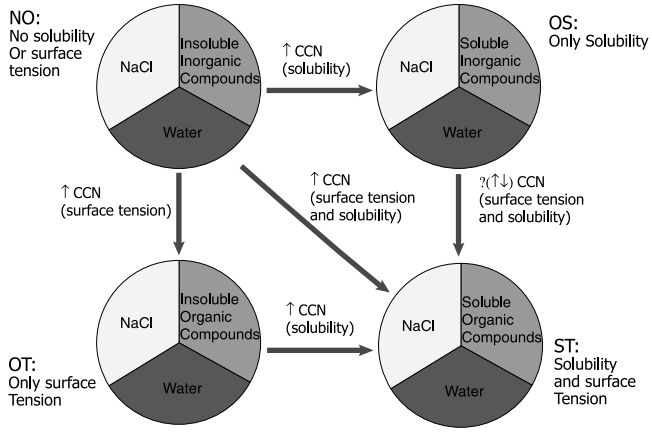

Figure 1. Schematic diagram showing surface tension and solubility effects on CCN concentrations. The chemical compositions of the four particle types are varied as indicated while holding particle mass and density constant. The changes in CCN concentrations are derived from the same initial size distribution.

[7] During fog events, the interstitial aerosol and fog droplets were sampled by an inertial impactor and a Counterflow Virtual Impactor (CVI), respectively [*Noone et al.*, 1992]. The droplet volume size distributions were measured by two PMS Forward Scattering Spectrometer Probes (FSSP). The accumulation-mode (dry diameter range 0.10–1.0 μm) size distributions of the dry interstitial and residual aerosol were determined by Optical Particle Counters (OPCs) after sampling [*Noone et al.*, 1992].

[8] Ammonium nitrate (NH_4NO_3) and ammonium sulfate ($(NH_4)_2SO_4$) each accounted for approximately half of inorganic aerosol mass in the Po Valley [*Hallberg et al.*, 1992]. *Decesari et al.* [2001] measured carbonaceous aerosol in the Po Valley in 1998–1999 using HNMR and TOC characterization of water-soluble organic compounds [*Decesari et al.*, 2000] and found that 47% of organic mass collected in November was water soluble. There were two types of aerosol with different hygroscopicity: the less and more hygroscopic particles. The average hygroscopic growth factors of both types of aerosol were measured using a Tandem Differential Mobility Analyzer (TDMA) to be 1.1 for the less hygroscopic particles and 1.5 for the more hygroscopic particles, both at 85% relative humidity [*Svenningsson et al.*, 1992].

[9] The fog was represented as a parcel containing detailed aerosol dynamics, including condensation, coagulation, and dry and wet deposition [*Russell and Seinfeld*, 1998]. As a result of gravitational settling, wet deposition of fog droplets removed dry aerosol mass and associated liquid water from the atmosphere. The settling velocity of wet particles was calculated according to *Seinfeld and Pandis*

[1998]. The dry diameter range of 0.004–10 μm was divided into 40 logarithmically spaced equal size bins. The initial size distribution of aerosol was made up of two lognormal distributions: an accumulation mode fitted to prefog measurements [*Noone et al.*, 1992] (N (number concentration): 5520 cm^{-3}; D_p (mean diameter): 0.185 μm; log(σ) (standard deviation): 0.188) and a nucleation mode typical of rural aerosol [*Jaenicke*, 1993] (N: 6650 cm^{-3}; D_p: 0.015 μm; log(σ): 0.225). The size distributions of the less and more hygroscopic particles were determined from their number fractions measured by *Svenningsson et al.* [1992].

[10] The chemical composition of aerosol was assumed to be independent of size due to the lack of size-resolved composition information. The inorganic mass fractions of the less and more hygroscopic particles were estimated to be 15% and 80%, respectively, based on the measured hygroscopic growth factors. For both types of aerosol, the inorganic fraction was composed of 50% NH_4NO_3 and 50% $(NH_4)_2SO_4$. The organic fraction contained 53% insoluble and 47% soluble compounds. The organic fraction of aerosol contains a large number of compounds, which vary in chemical structures and properties (e.g., solubility), and cannot be effectively represented by one model compound. The seven model compounds (i.e., pinonaldehyde, levoglucosan, catechol, nonandioic acid, 3-hydroxybutanoic acid, 3-hydroxybenzoic acid, and fulvic acid) based on the measured functional group composition of organic aerosol [*Fuzzi et al.*, 2001] were used to represent the water soluble organic mass. Although more than one set of model compounds can be derived from the measured functional group composition, the model compounds used in this study were chosen on the basis of their presence in ambient aerosol. Two hypothetical compositions (i.e., highly soluble and insoluble) were used to assess the model sensitivity to chemical composition. The thermodynamic model developed by *Ming and Russell* [2002] interpolated between measured interactions between organic compounds to calculate the solution activities of aqueous solutions containing NH_4NO_3, $(NH_4)_2SO_4$, and organic compounds. Because there are no published dissociation constants available for the compounds used in the model [*Velezmoro and Meirelles*, 1998], we have assumed that the soluble organic compounds do not dissociate. The measured surface tension of bulk fog water was assumed to describe the droplet average surface tension dependence on organic concentration [*Facchini et al.*, 2000].

[11] The HNO_3 condensation rate was calculated according to the approaches proposed by *Makar et al.* [1998] and *Mozurkewich* [1993]. The measured mass accommodation coefficients of HNO_3 ranged from 0.07 at 293 K to 0.19 at 268 K [*DeMore et al.*, 1994]. A value of 0.15 was interpolated at the temperature of interest for this study (around 275 K). The measured gas-phase concentrations of HNO_3 and NH_3 [*Facchini et al.*, 1992] were used in the model. The average concentration was approximately 8 neq m^{-3} for HNO_3 and 300 neq m^{-3} for NH_3. The aqueous-phase oxidation of SO_2 in the fog was negligible due to very low concentrations of SO_2 and oxidant species (O_3 and H_2O_2) during the experiment [*Facchini et al.*, 1992]. The water condensation rate was calculated following the approach described by *Seinfeld and Pandis* [1998].

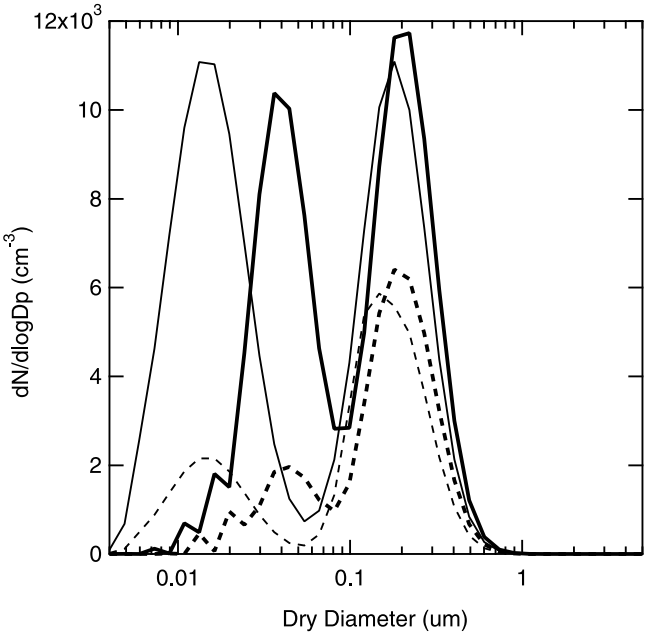

Figure 2. Size distribution of particles at 1900 LT (thin lines) and 2000 LT (thick lines). The distributions of the more hygroscopic particles are represented by dashed lines. The overall distributions of the more hygroscopic and less hygroscopic particles are represented by solid lines.

According to the latest measurement by *Li et al.* [2001], the mass and heat accommodation coefficients of water used in the model were 0.2 and 1, respectively.

3. Results

[12] Event 1 (10–11 November) and Event 4 (15–16 November) of the fog events observed in the Po Valley Fog Experiment of 1989 were simulated to compare their durations and LWC. Model results and sensitivities to some key factors are discussed in detail for Event 1. Both the surface tension and solubility effects of organic components (ST) are incorporated in the base case.

3.1. Base Case: Event 1

[13] Event 1 spanned 6 hours, which we divided into two consecutive periods: a prefog period (from 1900 to 2000 LT 10 November) and a fog period (from 2000 LT 10 November to 0100 LT 11 November).

3.1.1. Prefog Period

[14] The atmosphere remains below the cutoff relative humidity of 99% in the prefog period. For this condition, the distribution of water between ambient water vapor and particles is assumed to be at equilibrium [*Pandis et al.*, 1990]. This period is important for quantifying the growth of particles from condensable vapors.

[15] The size distributions of the less and more hygroscopic particles at the beginning and end of the prefog event are presented in Figure 2. As a result of high gas-phase concentrations of HNO_3 and NH_3, NH_4NO_3 is formed in particles. For the less hygroscopic particles, the diameter of the peak nucleation-mode concentration changes from 0.015 μm to 0.04 μm. The total particle number concentration in that mode decreases by 15% due to coagulation.

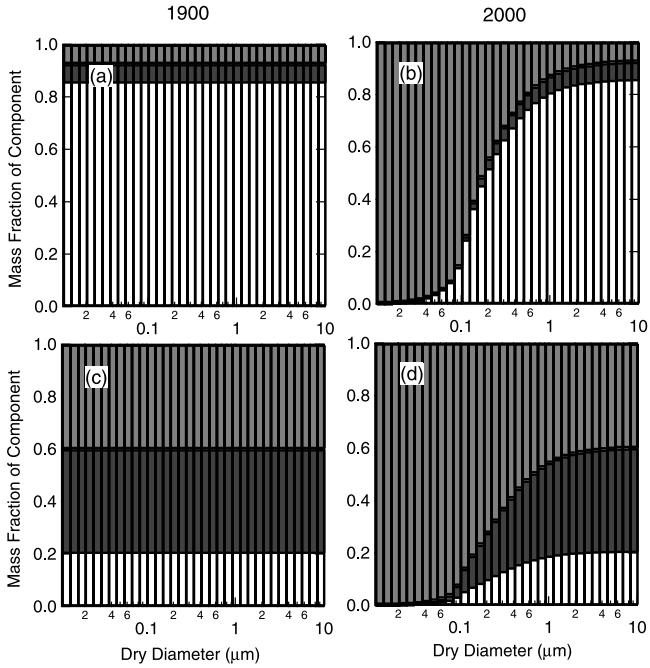

Figure 3. Fractions of NH_4NO_3 (gray column), $(NH_4)_2SO_4$ (black column), and organic species (white column) in (a) the less hygroscopic particles at 1900 LT, (b) the less hygroscopic particles at 2000 LT, (c) the more hygroscopic particles at 1900 LT, and (d) the more hygroscopic particles at 2000 LT in Event 1.

Condensation also shifts the distribution toward larger sizes in the accumulation mode, but to a lesser extent than in the nucleation mode. Similarly, the more hygroscopic particles experience growth in both modes. The diameter of the peak accumulation-mode concentration of the more hygroscopic particles shifts from 0.15 to 0.19 μm. Because the more hygroscopic particles have higher growth factors than the less hygroscopic particles with the same dry diameter at a given relative humidity, the surface area of the more hygroscopic particles that is available for condensation is larger, enhancing condensation.

[16] The size-resolved chemical compositions of both types of aerosol at the end of the prefog event (2000 LT) are plotted in Figure 3. For the less hygroscopic particles, NH_4NO_3, $(NH_4)_2SO_4$ and organic compounds initially account for 7.5%, 7.5% and 85% of total dry mass, respectively. At 2000 LT, the average mass fraction of NH_4NO_3 is approximately 95% for particles smaller than 0.10 μm and 10% for particles larger than 1 μm. In the accumulation mode, this fraction gradually decreases from 95% to 10%, as the particle size increases from 0.10 μm to 1 μm. The more hygroscopic particles follow a similar pattern. The average mass fraction of NH_4NO_3 for particles smaller than 0.10 μm increases from 40% at 1900 LT to 98% at 2000 LT, while it remains unchanged at 40% for particles larger than 1 μm. At 2000 LT, the fraction decreases almost linearly with the logarithmic dry diameter from 96% at 0.10 μm to 56% at 1 μm. At the start of the prefog period, the predicted concentrations are 889 neq m^{-3} (0.016 mg m^{-3}) for NH_4^+ and 402 neq m^{-3} (0.025 mg m^{-3}) for NO_3^-. After one hour of condensation, NH_4^+ increases to 1640 neq m^{-3} (0.030 mg m^{-3}) and NO_3^- to 1160 neq m^{-3} (0.072 mg m^{-3}). The predicted concentrations are within 50% of measurements [*Facchini et al.*, 1992].

[17] The hygroscopic growth factors of particles are dependent on chemical composition and ambient relative humidity. Figure 3 illustrates the considerable increase in the mass fraction of NH_4NO_3 for the submicron particles due to condensation. This change in chemical composition increases hygroscopicity as shown in Figure 4. For the less hygroscopic particles, the initial hygroscopic growth factor at 1900 LT is approximately 1.1 at 85% relative humidity. At 2000 LT, the growth factors are over 1.5 for particles smaller than 0.10 μm and unchanged for particles larger than 1 μm. The accumulation-mode particles have lower growth factors with increasing size. The increase in hygroscopicity is less significant for the more hygroscopic particles.

3.1.2. Fog Period

[18] The decrease in temperature causes relative humidity to reach supersaturation at 2000 LT. As shown in Figure 5a, the measured temperature profile describes clearly the cooling of air near the ground that causes fog formation while fluctuating within a range of ±1 K [*Wobrock et al.*, 1992]. Our model used the smooth temperature profile fitted to the measurements shown in Figure 5a because the fluctuations in the observations cause high-frequency changes for which the model would require excessive computational time. The temperature starts at 275.4 K at 2000 LT, and gradually decreases to 273.7 K at 0100 LT of the next day. The average cooling rate during the first two hours is 0.34 K hr^{-1}. The predicted LWC and supersaturation are plotted in Figures 5b and 5c. The predicted supersaturation quickly

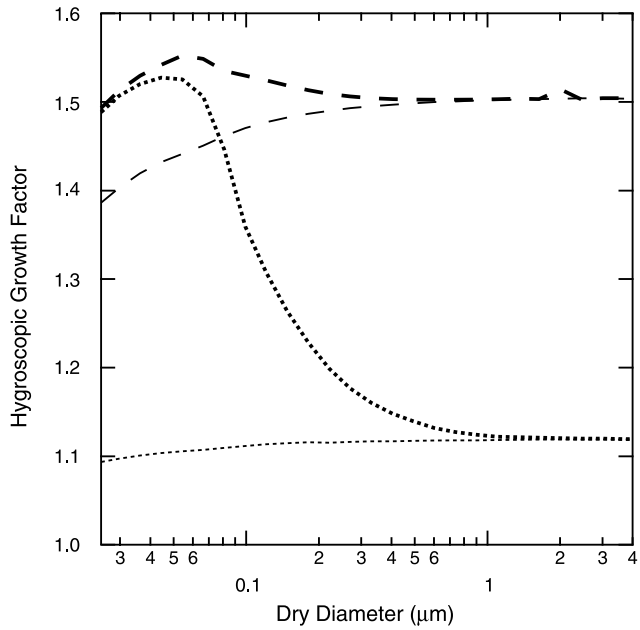

Figure 4. Predicted hygroscopic growth factors of the less (thick dotted line) and more (thick dashed line) hygroscopic particles at 2000 LT in Event 1. The predicted growth factors at 1900 LT are shown for the less (thin dotted line) and more (thin dashed line) hygroscopic particles.

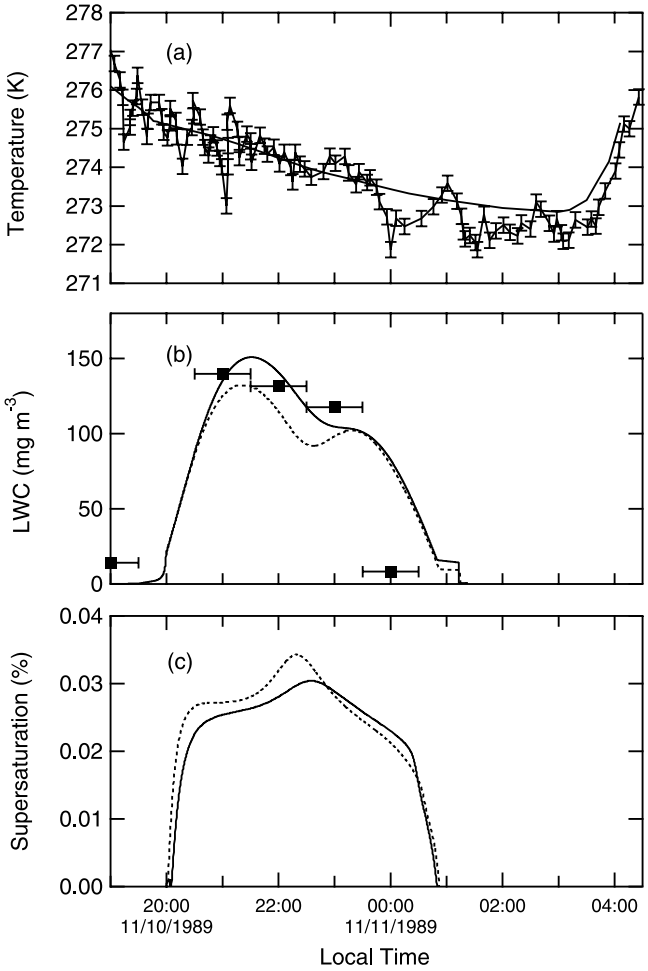

Figure 5. Temperature, liquid water content (LWC), and supersaturation in Event 1. (a) Thin solid line with error bars representing measured temperature [*Wobrock et al.*, 1992]. The smoothed temperature profile used in this study is represented by the thick solid line. (b) Measured LWC [*Fuzzi et al.*, 1992] represented by squares with error bars. The predicted LWC is shown for model runs that use the decreased droplet surface tension (the base case, ST) (thick solid line) and surface tension of pure water (the soluble organic without decreased droplet surface tension case, OS) (thick dotted line). (c) Predicted supersaturation corresponding to these two cases shown for the same runs as in Figure 5b.

reaches 0.025% at 2030 LT and then remains relatively constant until 2330 LT. During the same time period, the LWC rises from 19 mg m^{-3} at 2000 LT to 150 mg m^{-3} at 2130 LT. The fog dissipates after 2130 LT until the LWC drops below 10 mg m^{-3} at 0100 LT, signaling the end of the fog. The supersaturation increases to a maximum of 0.030% from 2130 to 2215 LT. After decreasing slowly to 0.022% at 0020 LT, the supersaturation drops rapidly back to 0% at 0050 LT.

[19] The cutoff diameter used to separate droplets from interstitial aerosol by the CVI was 6 μm in Event 1 [*Noone et al.*, 1992], making this value appropriate for being used as the droplet cutoff diameter in the model. As a result of increasing supersaturation, the predicted activation diameters of two types of aerosol decrease during the first hour of the fog period (from 2000 to 2100 LT) (Figure 6). The decrease is discontinuous because of the finite widths of size sections used in the model. The more hygroscopic particles as small as 0.40 μm can grow into droplets, while the less hygroscopic particles need to be larger than 0.49 μm. The average droplet number concentration is 149 cm^{-3}, including 20 cm^{-3} less hygroscopic and 129 cm^{-3} more hygroscopic particles.

[20] The residual particle fractions for the first hour of the fog period are shown in Figure 7. The more hygroscopic particles with dry diameter of 0.50 μm grow larger than 6 μm only after 2012 LT. Since no particles in that size bin are collected by the CVI from 2000 to 2012 LT, the calculated average residual particle fraction from 2000 to 2100 LT is 80%. For the less hygroscopic particles, the residual particle fraction increases to 63% at 0.60 μm, and further to 82% at 0.74 μm. All particles larger than 1.1 μm have 100% residual particle fraction. As compared to the less hygroscopic particles, the more hygroscopic particles as small as 0.40 μm are capable of activating into droplets and have a residual particle fraction of 56%. The fraction reaches 100% when the diameter exceeds 0.74 μm. The overall residual particle fractions are derived from averaging the fractions of both types of aerosol based on their number fractions. The predicted overall residual particle fractions are compared to the measured fractions [*Noone et al.*, 1992] in Figure 7. The comparison of the measured and predicted values is good, despite the potential for sampling artifacts associated with semivolatile organic

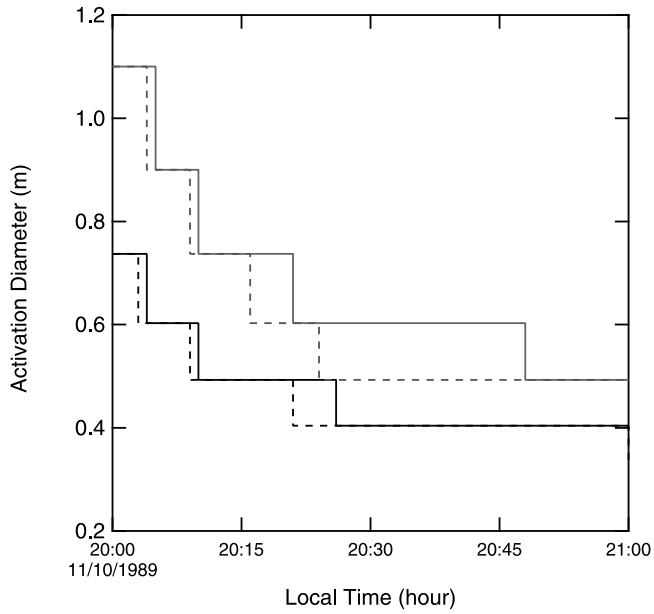

Figure 6. Activation diameters of the less and more hygroscopic particles from 2000 to 2100 LT in Event 1. The solid thick and thin lines represent the less and more hygroscopic particles in the base case (ST), respectively. The dotted thick and thin lines represent the less and more hygroscopic particles in the soluble organic without decreased droplet surface tension base (OS), respectively.

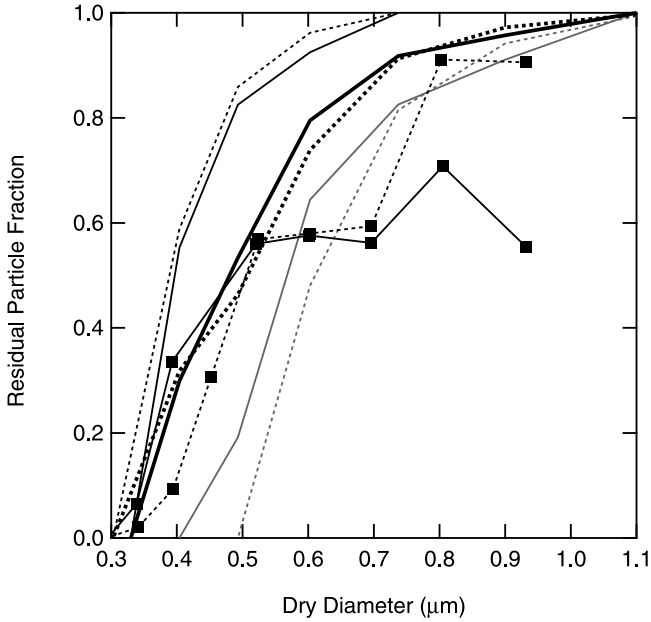

Figure 7. Average residual particle fractions from 2000 to 2100 LT in Event 1. The solid gray and black lines represent the residual particle fractions of the less and more hygroscopic particles in the bas case (ST), respectively. The dotted gray and black lines represent the residual particle fractions of the less and more hygroscopic particles in the soluble organic without decreased droplet surface tension base (OS), respectively. The thick solid and dotted lines represent the overall residual particle fractions of particles in the base (ST) and soluble organic without decreased droplet surface tension (OS) cases, respectively. The measured residual particle fractions in Event 1 and average residual particle fractions in all events are represented by the solid line with squares and by the dotted line with squares, respectively [*Noone et al.*, 1992].

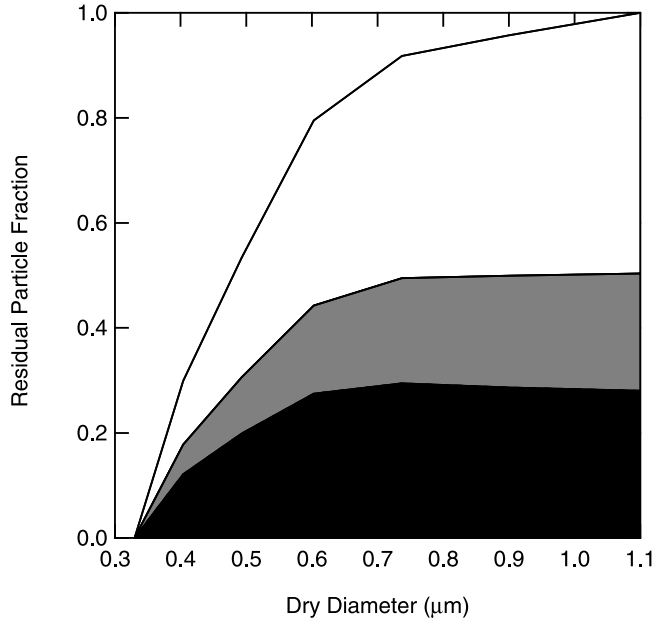

Figure 8. Contributions of NH_4NO_3 (white), $(NH_4)_2SO_4$ (gray), and organic compounds (black) to the average residual particle fractions from 2000 to 2100 LT in Event 1.

compounds. The model predictions agree well with measurements when the dry diameter is smaller than 0.50 μm, showing that the particles smaller than 0.33 μm cannot grow into droplets. There is a regime of relatively constant residual particle fraction between 0.50 and 0.70 μm in measurements, which had been attributed to the different activation diameters of the more and less hygroscopic particles [*Noone et al.*, 1992]: the more hygroscopic particles in the size range (0.50–0.70 μm) can grow into droplets, while the less hygroscopic particles in the same size range cannot. The predicted fog microphysics shows that the less hygroscopic particles as small as 0.49 μm grow into droplets. The residual particle fraction increases with dry diameter in the size range from 0.33 to 0.80 μm, without levelling off between 0.50 and 0.70 μm. Owing to the strong entrainment observed in Event 1, a significant fraction (over 30%) of particles larger than 0.80 μm did not grow into droplets [*Noone et al.*, 1992]. In other fog events with weaker entrainment, the measured residual particle fractions of particles larger than 0.80 μm were above 90% and consistent with the model. The large variability in the measured size distributions of residual particles prevents us from directly comparing the measured absolute number concentrations of residual particles to model results [*Noone et al.*, 1992]. The residual particle mass consists of 45% NH_4NO_3, 21% $(NH_4)_2SO_4$ and 34% organic compounds (Figure 8).

[21] The measured FSSP drop distribution [*Fuzzi et al.*, 1992] lies above the predicted average droplet volume size distribution at 2000 LT and below the predictions at 2200 LT as shown in Figure 9. Because the measure-

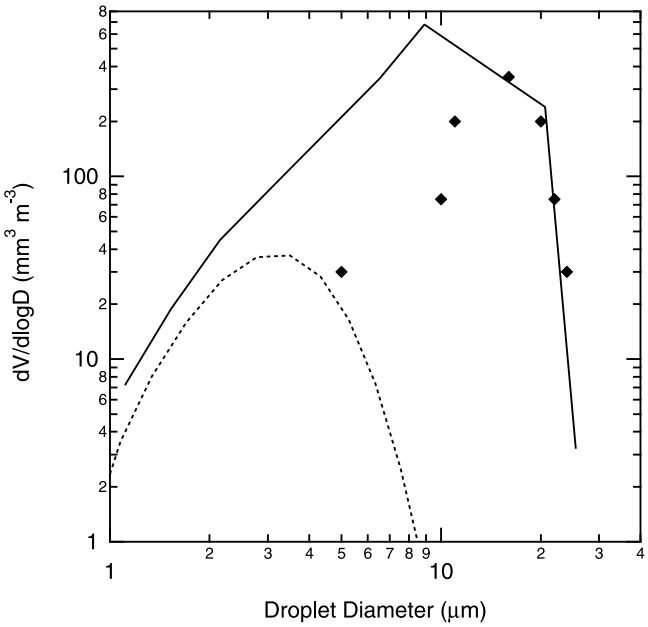

Figure 9. Droplet volume distributions at 2000 LT (dotted line) and 2200 LT (solid line) in Event 1. The average measurements by FSSP [*Fuzzi et al.*, 1992] are represented by diamonds.

ments represent an ensemble average of multiple parcels of particles over time, the bounding of the observed droplet concentrations within the predicted initial and fully formed drop distributions shows the consistency of the measured event with the model-predicted evolution.

3.2. Event 4

[22] Figure 10 summarizes the temperature, LWC and supersaturation in the simulation of Event 4. The model shows good agreement with the observed LWC. The temperature decreases at a rate of 0.88 K hr^{-1} in Event 4, faster than 0.34 K hr^{-1} in Event 1. The maximum LWC in Event 4 is 360 mg m^{-3}, more than twice as high as in Event 1. Despite the faster cooling rate, the maximum supersaturation in Event 4 is 0.032%, only slightly higher than 0.030% in Event 1.

3.3. Sensitivity Studies

[23] The droplet surface tension and chemical composition of particles are altered by the presence of organic components and condensation of soluble species. The total water content in the vapor and particle phases, between which the transport of water occurs through condensation and evaporation, is not conserved due to wet deposition, altering the relationship between LWC and supersaturation. We examine the effects of thermodynamic model assumptions, surface tension, chemical composition, condensation and wet deposition on fog formation. The sensitivity to the mass accommodation coefficient of droplets has been studied by other works (recently *Nenes et al.* [2002]), with which our results are consistent (see Appendix A).

3.3.1. Comparison of Water Activity and Surface Tension

[24] Organic compounds affect the activity of water by adding to the dissolved fraction and by changing the ideality of the solution behavior of the dissolved components. The organic fraction contributes organic ions to aqueous solutions through dissolution, increasing the mole fraction of dissolved solutes (x_i) and lowering the mole fraction of water (x_w). These dissolved organic ions interact with other dissolved ions, increasing or decreasing the ideality of the solution interactions, resulting in new values of activity coefficient (γ_w). Both soluble-fraction and solution-ideality effects are incorporated in the thermodynamic model [*Ming and Russell*, 2002], but here we illustrate the magnitude of each by considering them in turn. The no organic hygroscopicity case assumes that organic components do not dissolve, eliminating both effects. In this case, only inorganic salts contribute to the hygroscopic growth of particles. This assumption reduces hygroscopicity as a result of decreased ions compared to the base case. At the end of the prefog period, the dry diameters of particles are 3% smaller than in the base case. The corresponding droplet number concentration is 135 cm^{-3}, representing a 9% decrease from 149 cm^{-3} in the base case (Table 1). In the soluble organic without thermodynamic interaction case, we assume that organic components dissolve but do not change the solution ideality. The activity coefficient of water is held constant to exclude the effect of these dissolved organics on solution ideality in organic water interaction. In this case the water activity is reduced, and the particles grow 2% in dry diameter bigger than in the base case, increasing the surface area available for condensation by 6%. The resulting increased concentrations of NH_4NO_3 lead to a droplet number concentration of 158 cm^{-3}, 6% higher than 149 cm^{-3} in the base case (Table 1).

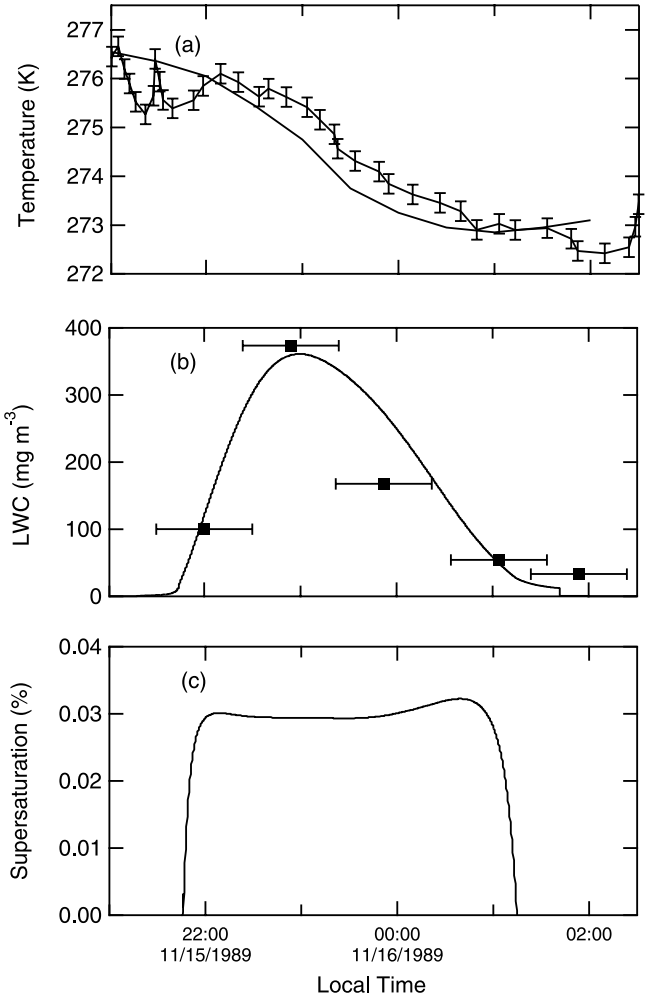

Figure 10. Same as Figure 5, but for Event 4.

[25] Surface-active organic compounds in aerosol expedite water condensation by lowering droplet surface tension below that of droplets formed from purely inorganic aerosol and that of pure water. In order to quantify the effect of the decreased droplet surface tension due to the organic part of the composition, the simulation of the fog period is rerun using the surface tension of pure water (the soluble organic without decreased droplet surface tension case, OS). The results are compared with the base case (the soluble organic with decreased droplet surface tension case, ST) in Figure 5. The higher surface tension in the soluble organic without decreased droplet surface tension case slows down water condensation because it enhances the water activity in droplets due to the Kelvin effect. The LWC in the soluble organic without decreased droplet surface tension case reaches a maximum of 132 mg m^{-3} at 2115 LT as compared to 150 mg m^{-3} in the base case. The maximum supersaturation is 0.035% in the soluble organic without decreased droplet surface tension case compared to 0.030% in the base case. The higher supersaturation increases the water condensation rate. As shown in Figure 6, the more hygroscopic

Table 1. Sensitivity of Model Predictions to Surface Tension, Chemical Composition, Condensation, and Deposition

Case	LWC, mg m^{-3}	Maximum Supersaturation, %	Droplet Number Concentration, cm^{-3}	Δ Mass Fraction of Organic Compounds in Residual Particles,[a] %	Δ Number Fraction of Less Hygroscopic Particles in Residual Particles,[a] %
Base case (ST)	150	0.030	149	0	0
Equilibrium base case[b]	150	0.030	182	3	−7
No organic hygroscopicity	146	0.031	135	+6	+7
Soluble organic without thermodynamic interaction	156	0.028	158	−3	−5
Soluble organic without decreased droplet surface tension case (OS)	132	0.035	145	0	−7
Soluble inorganic case	145	0.031	135	−26	−4
Increased solubility case	153	0.030	156	−2	5
Insoluble organic case (OT)	145	0.030	147	0	−7
Insoluble organic without decreased droplet surface tension case (NO)	129	0.034	145	−4	−12
No condensation case	121	0.037	118	10	9
No deposition case	595	0.023	160	−2	−6
No drop deposition case	595	0.068	186	−4	2

[a]Changes are relative to the base case.
[b]In equilibrium-based calculations, particles are counted as droplets when the fog supersaturation exceeds the corresponding critical supersaturation. (In kinetic-based calculations, the cutoff diameter is fixed at 6 μm.)

particles in the soluble organic without decreased droplet surface tension case grow faster than in the base case because the effect of the increased supersaturation outweighs that of the increased surface tension. The effect of the increased surface tension is stronger for the less hygroscopic particles due to their higher organic fractions than for the more hygroscopic particles. Consequently, the growth of the less hygroscopic particles in the soluble organic without decreased droplet surface tension case is delayed compared to the base case (Figure 6). The residual particle fractions in the soluble organic without decreased droplet surface tension case show the same trend as in the base case in Figure 7. The average droplet number concentration in the soluble organic without decreased droplet surface tension case is 145 cm^{-3}, only slightly lower than 149 cm^{-3} in the base case (Table 1).

[26] Four cases with different chemical compositions and surface tension are used to assess the surface tension and solubility effects on fog: the more hygroscopic particles composed of only inorganic salts (the soluble inorganic case); all organic components as malic acid (the increased organic solubility case); all organic components as long-chain alkanes (the insoluble organic case, OT); and all organic components as long-chain alkanes with the surface tension of pure water (the insoluble organic without decreased droplet surface tension case, NO). The model results are summarized in Figure 11 and Table 1. The substitution of the organic fraction of the more hygroscopic particles with inorganic salts increases the number of ions available for dissolution per unit dry particle mass and droplet surface tension at the same time. The effect of the increased droplet surface tension, which retards water condensation and reduces the droplet number concentration, outweighs the gain in the droplet number concentration due to the increased solubility. The LWC in the soluble inorganic case increases at a rate 7% lower than in the base case. The average droplet number concentration in the soluble inorganic case is 135 cm^{-3}, 9% lower than 149 cm^{-3} in the base case.

[27] Malic acid has a smaller molecular weight than the compounds used in the base case, providing more organic ions per unit dry particle mass. The increased solubility effect gives rise to an average droplet number concentration of 156 cm^{-3}, 5% higher than the base case. Treating all organic components as long-chain alkanes reduces the ions available for dissolution to result in an average droplet number concentration of 147 cm^{-3}, 1% lower than the base case. The average droplet number concentration is 145 cm^{-3} in the insoluble organic without decreased droplet surface tension case, 3% lower than the base case. In the soluble inorganic case, the particles larger than 0.60 μm have higher residual fractions than those in the base case (Figure 12). This difference is attributed to the higher supersaturation in the soluble inorganic case than in the base case. The residual particle fractions in the increased organic solubility case are higher than in the base case, while the fractions in the insoluble organic case are lower. Similarly, the insoluble organic without decreased droplet surface tension case has the lowest fractions of the four cases.

3.3.2. Vapor Condensation

[28] The NH_4NO_3 condensation in the prefog period increases the inorganic fractions of both the more and less hygroscopic particles. In order to assess the effect of condensation on fog formation, we simulate Event 1 with the concentrations of nonwater precursor species (i.e., NO_2, SO_2 and NH_3) in equilibrium with particle composition so that there is no net condensation or evaporation of these species (the no condensation case). In the prefog period, the absence of condensation leaves the chemical composition of aerosol particles unchanged. The predicted LWC and supersaturation are compared with the base case in Figure 11. The no condensation case has a maximum LWC of 120 mg m^{-3}, considerably lower than 150 mg m^{-3} in the base case. After rising rapidly to 0.030%, the supersaturation in the no condensation case remains relatively constant until 2100 LT, and then peaks again at 0.037% at 2200 LT. Despite the higher residual particle fractions than the base case (Figure 12), the average droplet number concentration in the no condensation case is 118 cm^{-3}, lower than 149 cm^{-3} in the base case. The NH_4NO_3 condensation

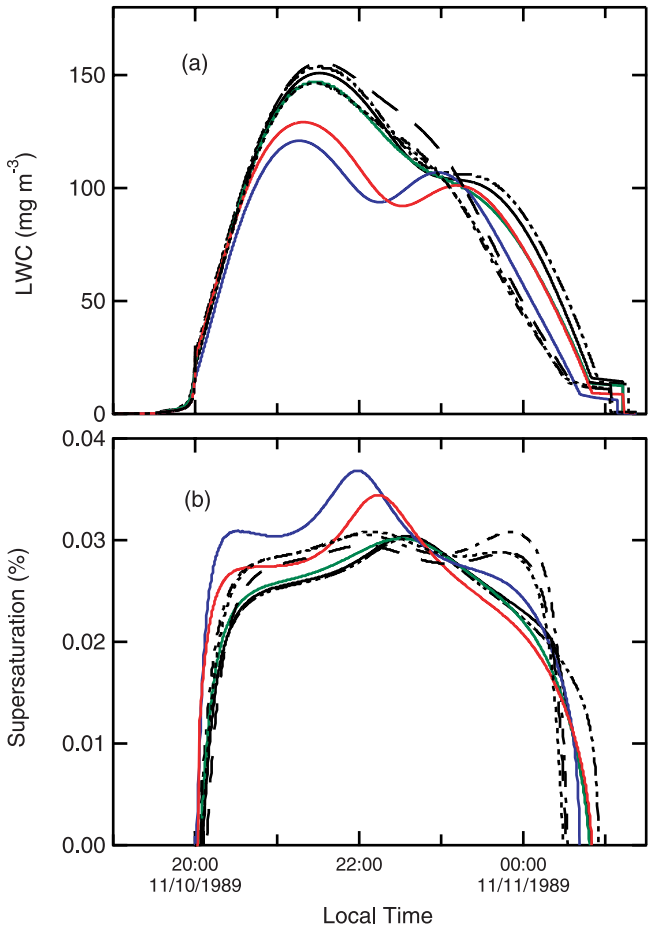

Figure 11. Influence of composition and condensation on the (a) predicted liquid water content (LWC) and (b) supersaturation in Event 1. The base (ST), no organic hygroscopicity, and soluble organic without thermodynamic interaction cases are represented by the black solid, dotted, and dashed lines, respectively. The soluble inorganic, increased solubility, insoluble organic (OT), and insoluble organic without decreased droplet surface tension (NO) cases are represented by the black dash-dotted, black dash-double-dotted, green solid, and red solid lines, respectively. The no condensation case is represented by the blue solid line.

increases the droplet number concentration by growing particles that were otherwise too small. The residual particle mass in the no condensation case consists of 28% NH_4NO_3, 28% $(NH_4)_2SO_4$ and 44% organic compounds (Table 1).

3.3.3. Wet Deposition

[29] Dry particle mass together with absorbed liquid water is removed from the atmosphere by wet deposition. This effect is studied with two schemes for wet deposition. The wet deposition of particles is turned off in the first scheme (the no deposition case), making the fog a closed system, in which the total water content and dry particle mass are conserved. Although the assumption of a closed system is not strictly applicable to any fog, a fog event of short duration (e.g., within 1 hour) is effectively closed given the negligible removal of particles and liquid water through wet deposition during the lifetime of the fog. The second scheme (the no drop deposition case) allows only dry particle mass to deposit, whereas the total water content is conserved based on the assumption that the liquid water removed by wet deposition is capable of evaporating back into the atmosphere. Figure 13 shows that both cases produce similar LWC, which increases continuously with decreasing temperature without causing dissipation. The conserved total water content in both cases gives rise to a maximum LWC of 595 mg m^{-3} at 0010 LT, much higher than 150 mg m^{-3} in the base case. The supersaturation in the no deposition case increases rapidly from 2000 to 2035 LT reaching 0.022%, and then starts to decrease gradually to 0.008% at 0100 LT. The fluctuation of increasing amplitude is characteristic of the supersaturation in the no drop deposition case. A maximum supersaturation of 0.066% is reached at 0050 LT (Table 1). The results highlight the important role of wet deposition in controlling the total water content in the vapor and particle phases. The fog supersaturation depends both on the total water content and LWC. If wet deposition is omitted, the model treats the total water content as constant, significantly overestimating LWC and droplet number concentration.

[30] Some processes other than wet deposition (e.g., advection) may also alter the total water content. The Po Valley studies employed single-point Eulerian sampling, which is insufficient for constraining advection. The good agreement shown by the predicted and measured LWC is consistent with wet deposition playing an important role in the fog evolution. This agreement does not preclude a contribution from advection.

4. Discussion

4.1. Surface Tension and Solubility Effects of Organic Components

[31] Surface-active organic compounds lower droplet surface tension [*Facchini et al.*, 2000]. We use an equilib-

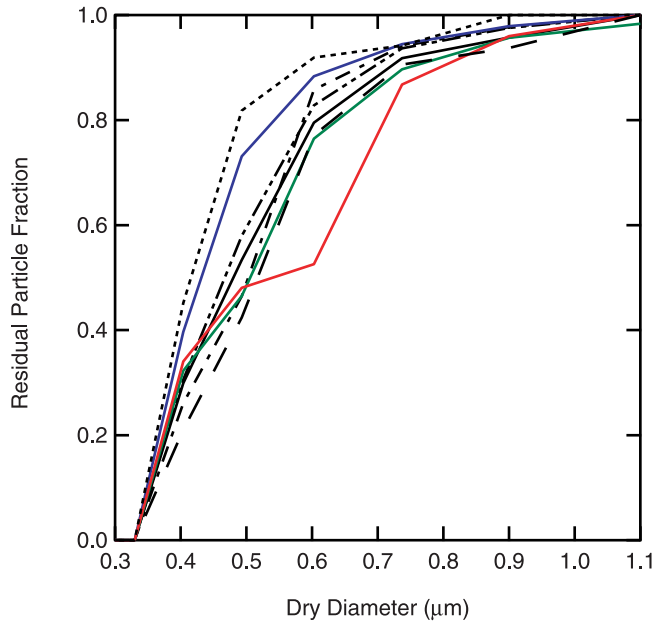

Figure 12. Influence of composition and condensation on the overall residual particle fractions in Event 1. The line scheme is the same as in Figure 10.

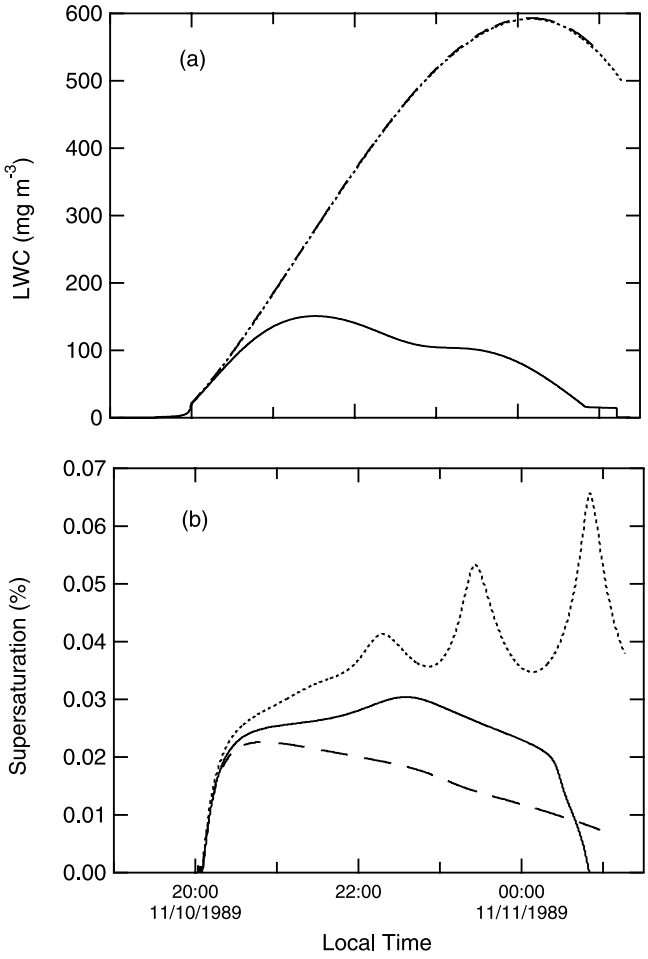

Figure 13. (a) Liquid water content (LWC) and (b) supersaturation in Event 1 using different schemes of wet deposition: the base (solid lines), no deposition (dashed lines), and no drop deposition (dotted lines) cases.

rium-based approach to calculate the droplet number concentrations at 0.030% from the chemical composition and size distribution of aerosol at the start of the fog event. According to this approach, a particle is counted as a droplet when the given supersaturation exceeds its critical supersaturation. *Mircea et al.* [2002] employed a similar method to estimate the influence of organic aerosol on CCN spectra for different types of aerosol. Our calculations reveal an average droplet number concentration of 607 cm^{-3} at 0.030% in the base case and 386 cm^{-3} in the soluble organic without decreased droplet surface tension case (Table 2). The decreased droplet surface tension has the effect of increasing the droplet number concentration by 57%. A similar equilibrium calculation with the typical chemical composition and size distribution of rural aerosol by *Mircea et al.* [2002] agrees with this estimate by showing that replacing the surface tension of pure water with the decreased droplet surface tension increases the droplet number concentration by 47% from 47 cm^{-3} in the soluble organic without decreased droplet surface tension case to 69 cm^{-3} in the base case (Table 2).

[32] The kinetic simulations show that the influence of the decreased droplet surface tension on fog formation is not as important as the equilibrium-based calculations suggest. For the more hygroscopic particles, the kinetic-based minimum activation diameters stay at 0.40 μm both in the soluble organic without decreased droplet surface tension case (OS) and in the base case (ST). For the less hygroscopic particles, the kinetic-based minimum activation diameters are 0.60 μm in the soluble organic without decreased droplet surface tension case and 0.49 μm in the base case (Figure 6). The average droplet number concentrations in the soluble organic without decreased droplet surface tension and base cases are 145 and 149 cm^{-3}, respectively. The increase caused by the decreased droplet surface tension is only 3%, considerably lower than the 57% increase from the equilibrium-based calculations. Although the decreased droplet surface tension lowers the critical supersaturation (S_c), it also causes droplets to grow larger than they would have grown under the impact of the surface tension of pure water, thus increasing LWC. The increase in LWC reduces the fog supersaturation (S). The reduced critical supersaturation (S_c) and the suppressed supersaturation (S) affect droplet growth simultaneously. The former causes particles to activate at a lower supersaturation, while the latter decreases the fog supersaturation. The effects of these two opposing factors largely cancel out any change in droplet number.

[33] *Nenes et al.* [2002] showed that the lowering of droplet surface tension due to surface-active organic components can increase the droplet number concentration by as

Table 2. Droplet Number Concentrations From Equilibrium-Based Calculations at a Supersaturation of 0.030%

	Mircea et al. [2002][a]		This Study	
Case	Droplet Number Concentration, cm^{-3}	Mass Fraction of Organic Compounds in Residual Particles, %	Droplet Number Concentration, cm^{-3}	Mass Fraction of Organic Compounds in Residual Particles, %
Base case (ST)	69	20	607	44
Soluble organic without decreased droplet surface tension case (OS)	47	20	386	25
Insoluble organic case (OT)	49	20	569	41
Insoluble organic without decreased droplet surface tension case (NO)	33	0	330	23

[a]The composition and size distribution of rural aerosol are based on the work of *Mircea et al.* [2002]. The aerosol mass contains 26% $(NH_4)_2SO_4$, 24% NH_4NO_3, 20% organic compounds, and 30% insoluble material. Insoluble material does not affect surface tension.

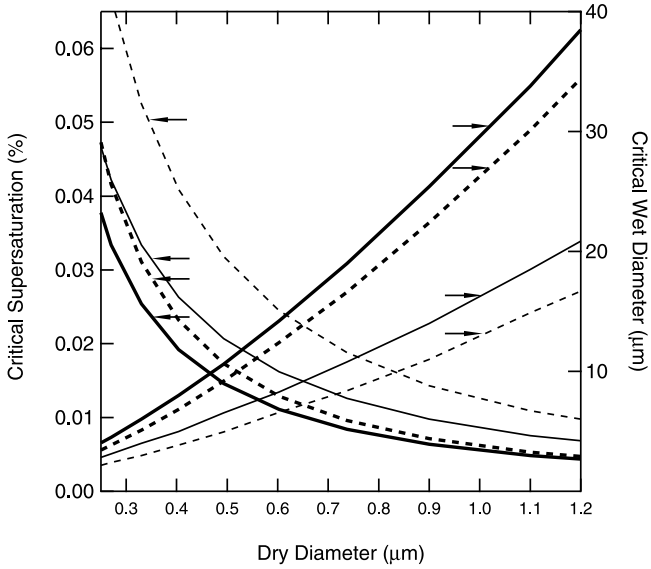

Figure 14. Critical supersaturation and wet diameter in the base case (ST) (solid lines) and in the soluble organic without decreased droplet surface tension (OS) case (dashed lines) for the less (thin lines) and more (thick lines) hygroscopic particles in Event 1.

much as 53% at an updraft velocity of 0.1 m s^{-1} for an urban aerosol of a typical size distribution. *Nenes et al.* [2002] assumed a typical trimodal lognormal distribution for urban aerosol: two nucleation modes which dominate particle numbers and one accumulation mode which accounts for a significant fraction of particle mass. By contrast, this work studies a measured size distribution from the Po Valley, composed of one nucleation mode (based on the typical size distribution of rural aerosol) and one accumulation mode (based on field measurements), both of which contribute comparable numbers of particles. The important role of surface tension shown by *Nenes et al.* [2002] is sensitive to the initial size distribution. The mode centered at 0.054 μm dominates droplet number concentrations at low to moderate updraft velocities (0.02–0.5 m s^{-1}) by *Nenes et al.* [2002], while most droplets in our Po Valley fog study are attributable to an accumulation mode at 0.20 μm. The large difference in the importance of organic surface tension effects on droplet numbers between our results and those of *Nenes et al.* [2002] is due to the different size distributions [*Noone et al.*, 1992].

[34] Comparing the insoluble organic case (OT) with the base case (ST) provides an assessment of the solubility effect of organic components on fog formation. As shown by the equilibrium-based calculations of *Mircea et al.* [2002] (Table 2), the droplet number concentration in the base case is 69 cm^{-3}, 41% higher than 49 cm^{-3} in the insoluble organic case. For comparison, the dissolution of the soluble organic compounds increases droplet number concentration by only 7% according to the equilibrium-based calculations of this study (569 cm^{-3} in the insoluble organic case and 607 cm^{-3} in the base case) (Table 2). The difference between our 7% change and the 41% change of *Mircea et al.* [2002] results largely from the hypothesis made by *Mircea et al.* [2002] that the low- and high-molecular-weight organic compounds contribute 3 and 5 ions per molecule, compared to our assumption of one ion per molecule. The kinetic simulations show that the average droplet number concentration is insensitive to the relatively weak solubility effect of organic components, increasing by only 1% (147 cm^{-3} in the insoluble organic case and 149 cm^{-3} in the base case) (Table 1), compared to the 7% increase from the equilibrium-based calculations. The increased solubility of the organic fraction has two impacts on the growth of droplets, reducing the critical supersaturation (S_c) and causing droplets to grow larger than they would have. The latter lowers the fog supersaturation (S) by increasing LWC, partially cancelling out the gain in droplet number concentration due to the decreased critical supersaturation (S_c).

4.2. Kinetic and Equilibrium-Based Condensational Growth

[35] The Köhler equation describes the equilibrium of water between supersaturated vapor and droplets by quantifying the surface tension and solubility effects [*Seinfeld and Pandis*, 1998]. The calculated critical supersaturation for both types of particles in the soluble organic without decreased droplet surface tension case (OS) are compared to the base case (ST) in Figure 14. The lowering of droplet surface tension due to organic components reduces the critical supersaturation by on average 31% for the less hygroscopic particles and by 52% for the more hygroscopic particles.

[36] The characteristic timescale necessary for establishing the equilibrium between water vapor and droplets during activation is longer than the timescale available for the kinetic transport of water in some conditions [*Chuang et al.*, 1997]. The kinetic wet diameter in the base case (ST) is compared with the equilibrium wet diameter calculated from the Köhler equation in Figure 15. At supersaturations lower than the critical supersaturation S_c, the kinetic diam-

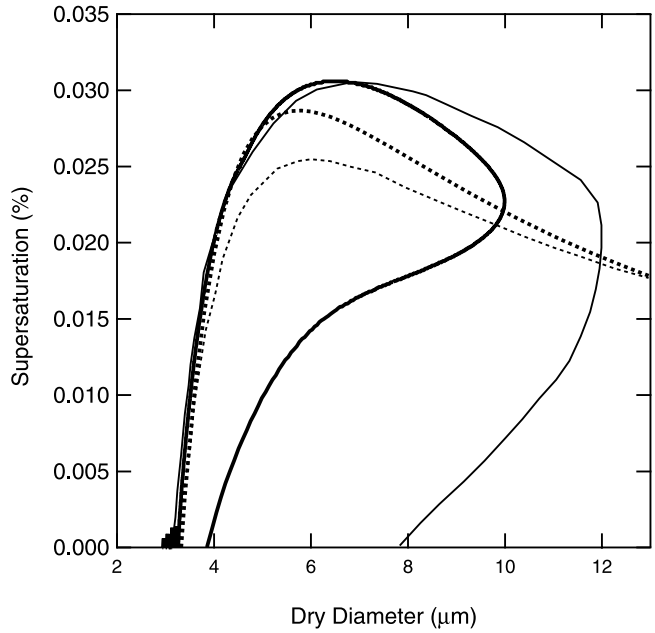

Figure 15. Kinetic (dotted lines) and equilibrium (solid lines) paths of a more hygroscopic particle with dry diameter of 0.33 μm in the base case (ST) (thin lines) and in the soluble inorganic case (thick lines) in Event 1.

eter of a droplet formed from a more hygroscopic particle with dry diameter of 0.33 μm is on average 9% smaller than the equilibrium diameter. The condensation growth continues as long as S is higher than the equilibrium supersaturation S_e at a specific droplet size since the difference $S - S_e$ provides the driving force for the kinetic transport of water between vapor and droplets and dictates its direction. The soluble inorganic case shows that the droplet begins to shrink at 10 μm as opposed to 12 μm in the base case due to the lack of organic effects, causing a 65% decrease in the average droplet diameter.

[37] The equilibrium activation diameters at the supersaturation from the kinetic simulations are calculated with the Köhler equation and compared to the kinetic activation diameters in Figure 16. For both types of particles, the equilibrium activation diameters agree with the kinetic ones from 2000 to 2015 LT when the supersaturation is below 0.015%. Then the kinetic activation diameters begin to fall behind the equilibrium ones since not enough time is available for water to reach equilibrium. These results are consistent with the comparisons of equilibrium and kinetic activation in previous works [*Chuang et al.*, 1997; *Russell et al.*, 2000]. The average droplet number concentration based on the equilibrium activation diameters is 182 cm^{-3}, representing an overestimation of 22% over the kinetic-based case (149 cm^{-3}) (Table 1). The evolution of the fog system studied here is clearly limited by the kinetic transport of water.

[38] The CVI serves as a good tool for selecting droplets bigger than a cutoff size (6 μm) from the interstitial particles. The same cutoff size was used to identify the model droplets. This comparison is independent of the activation state, since that cannot be directly measured. Other criteria used in the literature include that of *Frank et al.* [1998] who define activated particles measured by the Droplet Aerosol Analyzer (DAA) [*Martinsson*, 1996] as those bigger than predicted for an averaged dry particle size and an assumed composition.

5. Conclusions

[39] Our kinetic simulations with a Lagrangian-type parcel model that includes detailed aerosol dynamics predicted aerosol properties that are very similar to the field measurements in the Po Valley Fog Experiment of 1989. The organic fraction of aerosol mass was explicitly modeled as a mixture of seven soluble organic compounds [*Fuzzi et al.*, 2001], whose hygroscopic properties were based on a functional group model [*Ming and Russell*, 2002]. The measured decreased surface tension [*Facchini et al.*, 2000] was used to account for the presence of surface-active organic components. The simulated fog event had a maximum supersaturation of 0.030%, with minimum activation diameters of the less and more hygroscopic particles of 0.49 μm and 0.40 μm, respectively.

[40] Organic components increase the CCN efficiency of aerosol by decreasing droplet surface tension and by providing additional solute mass. Our simulations showed that the surface tension and solubility effects of organic components increase the average droplet number concentration by 3% and 1%, respectively. The thermodynamic equilibrium of particles containing inorganic ions and organic compounds determines their hygroscopic growth, and thus the surface area onto which soluble gases (i.e., HNO_3 and NH_3) can condense. The aqueous solutions formed in particles contain both inorganic salts and water-soluble organic compounds, and exhibit nonideality in water activity. Omitting the effect of the organic water interaction on water activity leads to an overestimation of hygroscopic growth and increases the average droplet number concentration by 6%. Condensation plays an important role in increasing the hygroscopicity of particles and making them more efficient for droplet formation. The mass transfer of HNO_3 and NH_3 to particles produces NH_4NO_3, increasing the average droplet number concentration by 26%. The presence of water-soluble organic compounds enhances condensation by increasing the hygroscopic growth of particles, causing an increase of 9% in the average droplet number concentration.

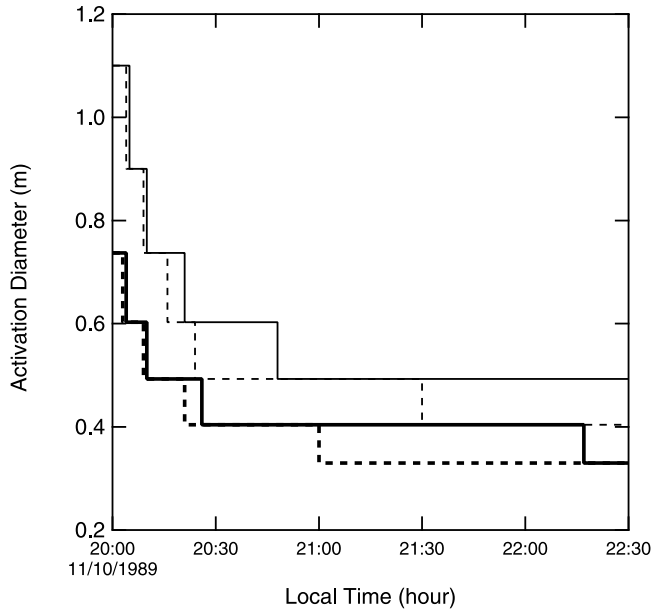

Figure 16. Activation diameters of the less and more hygroscopic particles from 2000 to 2230 LT in Event 1. The solid thin and thick lines represent the less and more hygroscopic particles using the kinetic simulation, respectively. The dashed thin and thick lines represent the less and more hygroscopic particles with the equilibrium-based calculation, respectively.

[41] The wet deposition of droplets is important in controlling the total water content in the vapor and particle phases, which determines the relationship between LWC and supersaturation. If wet deposition is omitted, the model significantly overestimates LWC and droplet number concentration and fails to predict the dissipation of fog as the temperature decreases. The predicted kinetic-based increases are considerably lower than the 57% increase due to the surface tension effect and the 7% increase due to the solubility effect of the equilibrium-based calculations. The less hygroscopic particles dominated by organic compounds contribute 14% of the droplet number concentration. Organic components account for 34% of the residual particle mass. Replacing 20% of the inorganic mass in the more hygroscopic particles with the organic mixture mea-

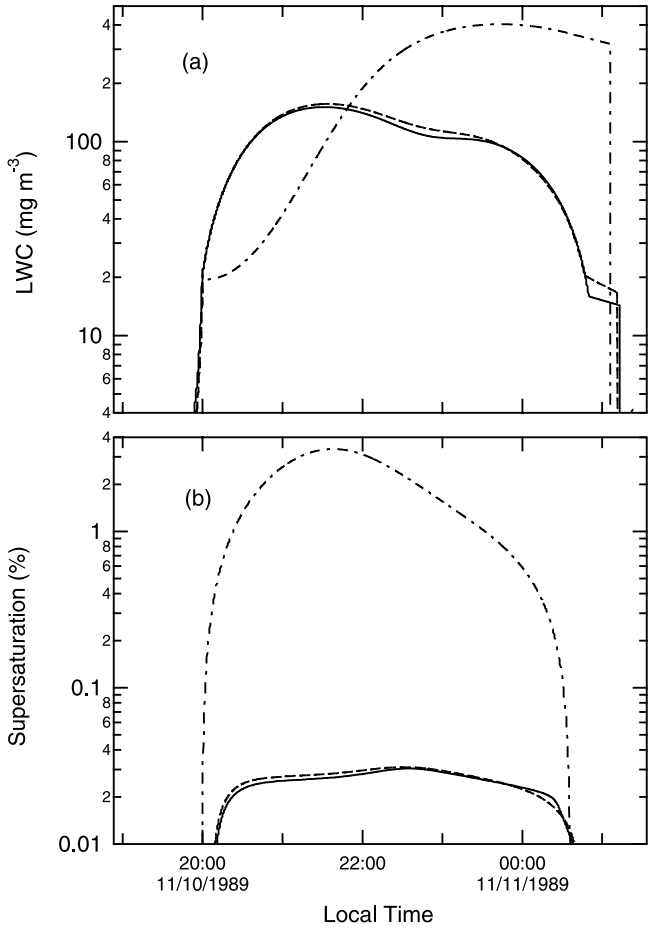

Figure A1. Influence of mass accommodation coefficient on the (a) predicted liquid water content (LWC) and (b) supersaturation in Event 1. Case A (dotted line) allows the coefficient to vary between 1×10^{-5} and 0.043 depending on the thickness of the organic film. Case B (dash-dotted line) and Case C (dashed line) set it to 1×10^{-5} and 0.043, respectively. The base case (solid line) uses 0.2.

sured in the Po Valley produces 7% more droplets. This case study highlights the role of organic compounds in the Po Valley, where measured NH_3 and NH_4NO_3 concentrations are consistently high. The detailed calculations of the thermodynamic behavior of model organic compounds are limited by the absence of measured molecular composition. Organic aerosol may play a more important role in fog formation in aerosol with a higher mass fraction of soluble organic compounds relative to soluble inorganic compounds.

Appendix A: Model Sensitivity to Mass Accommodation Coefficient

[42] *Feingold and Chuang* [2002] reported a mass accommodation coefficient of 1×10^{-5} with droplets coated by organic film and 0.043 in its absence [*Nenes et al.*, 2002]. Here we discuss the model sensitivity to this allowing the coefficient to vary between 1×10^{-5} and 0.043 depending on the thickness of the organic film (stable if >5 nm, otherwise unstable) [*Nenes et al.*, 2002] (Case A); Setting the mass accommodation coefficient to 1×10^{-5}, the lower bound (Case B); and an accommodation coefficient of 0.043 provides an upper bound (Case C). As shown in Figure A1 which plots the calculated liquid water content (LWC) and supersaturation (base case: solid line; Case A: dotted line; Case B: dash-dotted line; Case C: dashed line), Case A is almost identical to Case C, while Case B features unrealistically high LWC (max. 403 g m^{-3}) and supersaturation (max. 3.36%). Both Case A and Case C are very close to the base case which used 0.2. The predicted droplet number concentration in Case A is 149 cm^{-3}, only slightly lower than 150 cm^{-3} in the base case.

[43] As noted by *Nenes et al.* [2002], the film forming compounds (FFC) are only part of the insoluble organic fraction of aerosol mass. In our sensitivity study (specifically Case A), we assumed that all insoluble organic compounds (10% of the more hygroscopic particle mass and 37% of the less hygroscopic particle mass) can act as FFC. The FFC concentration of the more hygroscopic particles, which contribute most CCN, is still not high enough to cover droplets with organic films as thick as 5 nm, leaving the mass accommodation coefficient at 0.043. This explains the similarity between Case A and Case C.

[44] Owing to the weak cooling that governs fog formation in our study, the bigger particles (>0.5 μm) have enough time for condensational growth [*Chuang et al.*, 1997]. The reduced water condensation rate as a result of lowering the mass accommodation coefficient from 0.2 (the base case) to 0.043 (Case A) is not sufficient to affect the calculated droplet number concentration. The cooling of air parcels in the study by *Nenes et al.* [2002] is rapid, shortening the characteristic timescale necessary for reaching equilibrium [*Chuang et al.*, 1997] and leading to increases in supersaturation and droplet numbers.

[45] **Acknowledgments.** The authors are grateful to Kevin Noone and other participants in the Po Valley Fog Experiment for the data they have collected and published and for their advice. This study was supported under National Aeronautics and Space Administration grant NAG5-8676 and National Science Foundation grant ATM9732949.

References

Chuang, P. Y., R. J. Charlson, and J. H. Seinfeld (1997), Kinetic limitations on droplet formation in clouds, *Nature*, *390*, 594–596.

Corrigan, C. E., and T. Novakov (1999), Cloud condensation nucleus activity of organic compounds: A laboratory study, *Atmos. Environ.*, *33*, 2661–2668.

Cruz, C. N., and S. N. Pandis (1997), A study of the ability of pure secondary organic aerosol to act as cloud condensation nuclei, *Atmos. Environ.*, *31*, 2205–2214.

Decesari, S., M. C. Facchini, S. Fuzzi, and E. Tagliavini (2000), Characterization of water-soluble organic compounds in atmospheric aerosol: A new approach, *J. Geophys. Res.*, *105*, 1481–1489.

Decesari, S., M. C. Facchini, E. Matta, F. Lettini, M. Mircea, S. Fuzzi, E. Tagliavini, and J. P. Putaud (2001), Chemical features and seasonal variation of fine aerosol water-soluble organic compounds in the Po Valley, Italy, *Atmos. Environ.*, *35*, 3691–3699.

DeMore, W. B., S. P. Sander, C. J. Howard, A. R. Ravishankara, D. M. Golden, C. E. Kolb, R. F. Hampson, M. J. Molina, and M. J. Kurylo (1994), Chemical kinetics and photochemical data for use in stratospheric modeling, *Rep. JPL 94-26*, Jet Propul. Lab., Pasadena, Calif.

Duce, R. A., V. A. Mohnen, P. R. Zimmerman, D. Grosjean, W. Cautreels, R. Chatfield, R. Jaenicke, J. A. Ogren, E. D. Pellizzari, and G. T. Wallace (1983), Organic material in the global troposphere, *Rev. Geophys.*, *21*, 921–952.

Facchini, M. C., et al. (1992), The chemistry of sulfur and nitrogen species in a fog system—A multiphase approach, *Tellus, Ser. B.*, *44*, 505–521.

Facchini, M. C., S. Decesari, M. Mircea, S. Fuzzi, and G. Loglio (2000), Surface tension of atmospheric wet aerosol and cloud/fog droplets in

relation to their organic carbon content and chemical composition, *Atmos. Environ.*, *34*, 4853–4857.
Feingold, G., and P. Chuang (2002), Analysis of the influence of film-forming compounds on droplet growth: Implications for cloud microphysical processes and climate, *J. Atmos. Sci.*, *59*, 2006–2018.
Frank, G., et al. (1998), Droplet formation and growth in polluted fogs, *Contrib. Atmos. Phys.*, *71*, 65–85.
Fuzzi, S., et al. (1992), The Po Valley fog experiment 989–An overview, *Tellus, Ser. B.*, *44*, 448–468.
Fuzzi, S., S. Decesari, M. C. Facchini, E. Matta, M. Mircea, and E. Tagliavini (2001), A simplified model of the water soluble organic component of atmospheric aerosols, *Geophys. Res. Lett.*, *28*, 4079–4082.
Hallberg, A., et al. (1992), Phase partitioning for different aerosol species in fog, *Tellus, Ser. B.*, *44*, 545–555.
Jaenicke, R. (1993), Tropospheric aerosols, in *Aerosol-Cloud-Climate Interactions*, edited by P. V. Hobbs, pp. 1–31, Academic, San Diego, Calif.
Li, Y. Q., P. Davidovits, Q. Shi, J. T. Jayne, C. E. Kolb, and D. R. Worsnop (2001), Mass and thermal accommodation coefficients of H_2O(g) on liquid water as a function of temperature, *J. Phys. Chem. A*, *105*, 10,627–10,634.
Lillis, D., C. N. Cruz, J. Collett, L. W. Richards, and S. N. Pandis (1999), Production and removal of aerosol in a polluted fog layer: Model evaluation and fog effect on PM, *Atmos. Environ.*, *33*, 4797–4816.
Makar, P. A., H. A. Wiebe, R. M. Staebler, S. M. Li, and K. Anlauf (1998), Measurement and modeling of particle nitrate formation, *J. Geophys. Res.*, *103*, 13,095–13,110.
Martinsson, B. G. (1996), Physical basis for a droplet aerosol analysing method, *J. Aerosol Sci.*, *27*, 997–1013.
Middlebrook, A. M., D. M. Murphy, and D. S. Thomson (1998), Observations of organic material in individual marine particles at Cape Grim during the First Aerosol Characterization Experiment (ACE 1), *J. Geophys. Res.*, *103*, 16,475–16,483.
Ming, Y., and L. M. Russell (2002), Thermodynamic equilibrium of organic-electrolyte mixtures in aerosol particles, *AIChE J.*, *48*, 1331–1348.
Mircea, M., M. C. Facchini, S. Decesari, S. Fuzzi, and R. J. Charlson (2002), The influence of the organic aerosol component on CCN supersaturation spectra for different aerosol types, *Tellus, Ser. B.*, *54*, 74–81.
Mozurkewich, M. (1993), The dissociation-constant of ammonium-nitrate and its dependence on temperature, relative-humidity and particle-size, *Atmos. Environ., Part A*, *27*, 261–270.
Nenes, A., R. J. Charlson, M. C. Facchini, M. Kulmala, A. Laaksonen, and J. H. Seinfeld (2002), Can chemical effects on cloud droplet number rival the first indirect effect?, *Geophys. Res. Lett.*, *29*(17), 1848, doi:10.1029/2002GL015295.
Noone, K. J., et al. (1992), Changes in aerosol size and phase distributions due to physical and chemical processes in fog, *Tellus, Ser. B.*, *54*, 489–504.
Pandis, S. N., J. H. Seinfeld, and C. Pilinis (1990), Chemical-composition differences in fog and cloud droplets of different sizes, *Atmos. Environ., Part A*, *24*, 1957–1969.
Rogge, W. F., M. A. Mazurek, L. M. Hildemann, G. R. Cass, and B. R. T. Simoneit (1993), Quantification of urban organic aerosols at a molecular-level—Identification, abundance and seasonal-variation, *Atmos. Environ., Part A*, *27*, 1309–1330.
Russell, L. M., and J. H. Seinfeld (1998), Size- and composition-resolved externally mixed aerosol model, *Aerosol Sci. Technol.*, *28*, 403–416.
Russell, L. M., K. J. Noone, R. J. Ferek, R. A. Pockalny, R. C. Flagan, and J. H. Seinfeld (2000), Combustion organic aerosol as cloud condensation nuclei in ship tracks, *J. Atmos. Sci.*, *57*, 2591–2606.
Seinfeld, J. H., and S. N. Pandis (1998), *Atmospheric Chemistry and Physics*, John Wiley, Hoboken, N. J.
Svenningsson, I. B., H. C. Hansson, A. Wiedensohler, J. A. Ogren, K. J. Noone, and A. Hallberg (1992), Hygroscopic growth of aerosol-particles in the Po valley, *Tellus, Ser. B.*, *44*, 556–569.
Velezmoro, C. E., and A. J. A. Meirelles (1998), Water activity in solutions containing organic acids, *Dry Technol.*, *16*, 1789–1805.
Wobrock, W., et al. (1992), Meteorological characteristics of the Po Valley fog, *Tellus, Ser. B.*, *44*, 469–488.
Wyzga, R. E., and L. J. Folinsbee (1995), Health effects of acid aerosols, *Water Air Soil Pollut.*, *85*, 177–188.

Y. Ming, Geophysical Fluid Dynamics Laboratory, Princeton Forrestal Campus, Princeton, NJ 08542, USA. (yi.ming@noaa.gov)
L. M. Russell, Scripps Institution of Oceanography, University of California, San Diego, Mail Code 0221, 9500 Gilman Drive, La Jolla, CA 92093-0221, USA. (lmrussell@ucsd.edu)